ACS Combinatorial Science

RESEARCH ARTICLE

pubs.acs.org/acscombsci

Combinatorial Materials Research Applied to the Development of New Surface Coatings XV: An Investigation of Polysiloxane Anti-Fouling/Fouling-Release Coatings Containing Tethered Quaternary Ammonium Salt Groups

Partha Majumdar,[*,†] Elizabeth Crowley,[†] Maung Htet,[†] Shane J. Stafslien,[†] Justin Daniels,[†] Lyndsi VanderWal,[†] and Bret J. Chisholm[†,‡]

[†]The Center for Nanoscale Science and Engineering, North Dakota State University, 1805 Research Park Drive, Fargo, North Dakota 58102, United States

[‡]Department of Coatings and Polymeric Materials, North Dakota State University, 1735 Research Park Drive, Fargo, North Dakota 58102, United States

Supporting Information

ABSTRACT: As part of ongoing efforts aimed at the development of extensive structure−property relationships for moisture-curable polysiloxane coatings containing tethered quaternary ammonium salt (QAS) moieties for potential application as environmental friendly coatings to combat marine biofouling, a combinatorial/high-throughput (C/HT) study was conducted that was focused on four different compositional variables. The coatings that were investigated were derived from solution blends of a silanol-terminated polydimethylsiloxane (HO-PDMS-OH), QAS-functional alkoxysilane, and methyltriacetoxysilane. The compositional variables investigated were alkoxysilane functionality of the QAS-functional silane, chain length of the monovalent alkyl group attached to the QAS nitrogen atom, concentration of the QAS-functional alkoxysilane, and molecular weight of the HO-PDMS-OH. Of these variables, the composition of the alkoxysilane functionality of the QAS-functional silane was a unique variable that had not been previously investigated. The antifouling (AF) and fouling-release (FR) characteristics of the 24 unique coating compositions were characterized using HT assays based on three different marine microorganisms, namely, the two bacteria, *Cellulophaga lytica* and *Halomonas pacifica*, and the diatom, *Navicula incerta*. Coatings surfaces were characterized by surface energy, water contact angle hysteresis, and atomic force microscopy (AFM). A wide variety of responses were obtained over the compositional space investigated. ANOVA analysis showed that the compositional variables and their interactions significantly influenced AF/FR behaviors toward individual marine microorganisms. It was also found that utilization of the ethoxysilane-functional QASs provided enhanced AF character compared to coatings based on methoxysilane-functional analogues. This was attributed to enhanced surface segregation of QAS groups at the coating-air interface and confirmed by phase images using AFM.

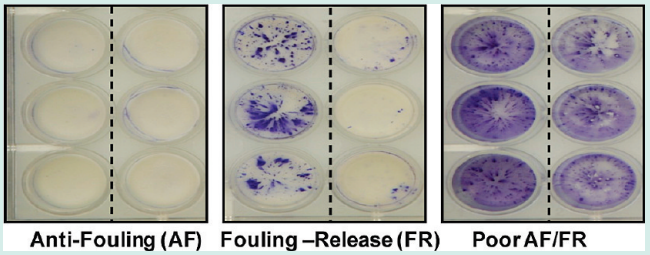

KEYWORDS: high-throughput, quaternary ammonium salt, polysiloxane, antifouling, fouling-release

INTRODUCTION

Marine biofouling, which is defined as the undesirable accumulation of microorganisms, plants, and animals on artificial surfaces immersed in seawater, is a major problem for surfaces such as ship hulls, aquaculture cages, and pipelines.[1−5] Biofouling on ship hulls increases surface roughness which causes higher hydrodynamic friction leading to increased fuel consumption, increased frequency of dry-docking, initiation of corrosion, and the introduction of invasive species to new environments.[1,3,4] Biofouling of aquaculture framings causes an estimated 20% increase in the cost of fish production because of the necessity for cleaning operations.[2]

The process of biofouling is generally believed to occur in multiple stages with significant overlap between the stages.[1,5] The first stage is the formation of a conditioning film within a minute of water immersion because of the settlement of organic molecules, such as proteins and polysaccharides. Next, within a day, bacteria and single-cell diatoms settle on this modified surface to form a microbial biofilm which promotes the accumulation of algal spores, barnacle cyprids, and marine fungi. In the final stage, the settlement and the growth of larger marine invertebrates together with the growth of macroalgae results in macrofouling.

More than 4,000 species of marine organisms have been identified over fouled surfaces.[1,3] These species differ in their mechanism of adhesion to substrates as well as in their adhesive

Received: January 12, 2011
Revised: March 22, 2011
Published: April 11, 2011

composition. Considering the diversity of fouling-organisms, it can be understood that the creation of an effective coating to combat biofouling is a considerable technical challenge.

Historically, the most effective antifouling (AF) coatings have been based on leachable copper and tin biocides with tributyltin-based, self-polishing acrylate coatings being the most effective.[6,7] Unfortunately, these biocide-releasing coatings also kill nontarget organisms and can accumulate in harbors causing detrimental changes to the aquatic environment.[8,9] Thus, to protect the marine environment, the International Maritime Organization in October 2001 banned new use of tributyltin-based paints effective January 1, 2003 and mandated replacement of tributyltin-based paints on ships effective January 1, 2008.[1,3]

As a result of continued environmental concerns related to biocide-releasing marine coatings, considerable effort has gone into the development of nontoxic replacements. Polysiloxane coatings with "easy-release" characteristics have been reported by various researchers and are commercially available as "fouling-release" (FR) coatings.[10−12] More recently, other approaches have been investigated for the production of nontoxic marine coatings.[13−18] Krishnan et al. reported that amphiphilic block copolymers with semifluorinated, liquid-crystalline side-chains showed good release of *Ulva* sporelings.[13] Statz et al. modified titanium substrates with methoxy-terminated poly(ethylene glycol)-L-3,4-dihydroxyphenylalanine copolymers and showed that they were more effective than polydimethylsiloxane-based coatings in inhibiting settlement of diatoms and *Ulva* sporelings.[14] Microtopographic patterned surfaces were explored to understand the effect of topographical features on the settlement of marine organisms. Sharklet AF patterned surfaces developed by Carman et al. and inspired from shark skin showed low settlement of *Ulva* zoospores.[16,17] Several other approaches for the development of nontoxic marine coatings have been reported, and the topic has been recently reviewed by Webster and Chisholm.[19]

The authors have been investigating the development of environmentally friendly marine coatings using an approach based on chemically grafting or "tethering" biocidal moieties to a polysiloxane matrix.[20−22] The primary biocide moiety of interest has been quaternary ammonium salts (QASs). QASs are well-known to possess biocidal activity through a mechanism involving electrostatic and lipophilic interactions with the cell wall of various microorganisms.[23−25] Surfaces coated with QAS-containing polymers have been shown to kill a wide range of microorganisms including Gram-positive bacteria, Gram-negative bacteria, yeasts, and molds.[22,25−27] Kugler et al. reported on the mechanistic aspects of QAS-functional surfaces.[28] According to their findings, the effectiveness of a QAS-functional surface largely depends on QAS concentration. For a given microorganism, a threshold QAS charge-density must be surpassed to obtain antimicrobial activity. The threshold QAS charge density was found to vary with the species of bacterium as well as the metabolic state of the bacterium. Murata et al. reported that antimicrobial efficacy of surfaces derived from QAS-functional polymer brushes was dependent on surface charge-density but independent of molecular weight of the polymer brushes.[29]

As shown in Figure 1, the QAS-functional coatings being investigated by the authors are based on solution blends of a silanol-terminated poly(dimethylsiloxane) (HO-PDMS-OH), a QAS-functional alkoxysilane, and the cross-linker, methyltriacetoxysilane (MeTAS). Previous results have shown that the effectiveness of these moisture-curable systems as marine

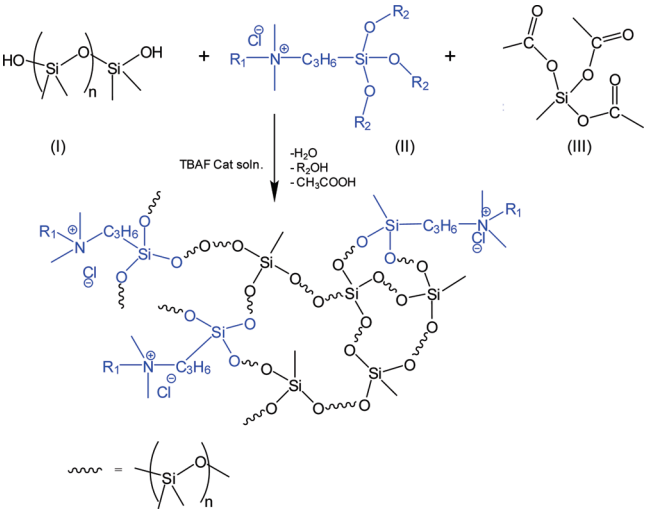

Figure 1. Schematic illustrating the formation of the cross-linked network containing tethered QAS groups. TBAF is tetrabutylammonium fluoride.

coatings depends strongly on compositional variables which include the concentration of the QAS-functional alkoxysilane, the length of the alkyl chain attached to the nitrogen atom (R_1 in Figure 1), and the molecular weight of the HO-PDMS-OH.[20,22] A correlation between coating surface morphology and both AF and FR characteristics was observed as part of this prior research. In general, compositions that displayed an AF effect and/or enhanced FR properties possessed a heterogeneous surface morphology. The generation of a heterogeneous surface morphology was dependent on complex interactions between the various compositional variables investigated. This paper describes further investigations of the compositional space described in Figure 1 with particular emphasis on the effect of the chemical structure of the alkoxysilane groups (R_2 in Figure 1). A combinatorial/high-throughput (C/HT) approach was applied to the investigation to enable multiple variables to be probed simultaneously and efficiently.[30−34]

EXPERIMENTAL PROCEDURES

Materials. Table S1 in the Supporting Information describes the starting materials used for the investigation. All the reagents were used as received. The marine bacterium *Halomonas pacifica* 27122 was received from the American Type Culture Collection. The marine bacterium *Cellulophaga lytica* was generously provided by Dr. Michael Hadfield of the Kewalo Marine Laboratory, University of Hawaii. The marine microalgae diatom *Navicula incerta* was generously provided by Dr. Maureen Callow, School of Biosciences, University of Birmingham, U.K. Artificial seawater (ASW) was prepared by dissolving 38.5 g of sea salts (Sigma-Aldrich) into 1 L of deionized water. Bacterial biofilm growth medium (BGM) consisted of 0.1 g of yeast extract and 0.5 g of dextrose (*H. pacifica*) or 0.5 g of peptone (*C. lytica*) per 1 L of ASW. Algal growth medium (F/2) consisted of 1 L of ASW supplemented with nutrients from Guillard's F/2 medium.[35] BGM, F/2, and ASW were filter sterilized with 0.2 μm vacuum-cap filters.

Synthesis of Alkoxysilane-Functional Quaternary Ammonium Salts (QASs). Alkoxysilane-functional QASs were synthesized by reacting a trialkoxysilane-functional alkyl halide with an

Table 1. Compositions of Coating Solutions Prepared for the Investigation[a]

coating	HO-PDMS-OH	alkoxysilane-functional QAS	QAS (mol X 10^3)	wt of QAS soln.	toluene
49K-C14-TMS-0.20	49K-PDMS	Q-C14-TMS	1.0	0.88	1.25
49K-C16-TMS-0.20	49K-PDMS	Q-C16-TMS	1.0	0.94	1.25
49K-C18-TMS-0.20	49K-PDMS	Q-C18-TMS	1.0	0.83	1.25
49K-C14-TES-0.20	49K-PDMS	Q-C14-TES	1.0	0.96	1.25
49K-C16-TES-0.20	49K-PDMS	Q-C16-TES	1.0	1.02	1.25
49K-C18-TES-0.20	49K-PDMS	Q-C18-TES	1.0	1.08	1.25
49K-C14-TMS-0.30	49K-PDMS	Q-C14-TMS	1.5	1.32	1.25
49K-C16-TMS-0.30	49K-PDMS	Q-C16-TMS	1.5	1.40	1.25
49K-C18-TMS-0.30	49K-PDMS	Q-C18-TMS	1.5	1.24	1.25
49K-C14-TES-0.30	49K-PDMS	Q-C14-TES	1.5	1.45	1.25
49K-C16-TES-0.30	49K-PDMS	Q-C16-TES	1.5	1.53	1.25
49K-C18-TES-0.30	49K-PDMS	Q-C18-TES	1.5	1.61	1.25
18K−C14-TMS-0.20	18K-PDMS	Q-C14-TMS	1.0	0.88	0.00
18K−C16-TMS-0.20	18K-PDMS	Q-C16-TMS	1.0	0.94	0.00
18K−C18-TMS-0.20	18K-PDMS	Q-C18-TMS	1.0	0.83	0.00
18K−C14-TES-0.20	18K-PDMS	Q-C14-TES	1.0	0.96	0.00
18K−C16-TES-0.20	18K-PDMS	Q-C16-TES	1.0	1.02	0.00
18K−C18-TES-0.20	18K-PDMS	Q-C18-TES	1.0	1.08	0.00
18K−C14-TMS-0.30	18K-PDMS	Q-C14-TMS	1.5	1.32	0.00
18K−C16-TMS-0.30	18K-PDMS	Q-C16-TMS	1.5	1.40	0.00
18K−C18-TMS-0.30	18K-PDMS	Q-C18-TMS	1.5	1.24	0.00
18K−C14-TES-0.30	18K-PDMS	Q-C14-TES	1.5	1.45	0.00
18K−C16-TES-0.30	18K-PDMS	Q-C16-TES	1.5	1.53	0.00
18K−C18-TES-0.30	18K-PDMS	Q-C18-TES	1.5	1.61	0.00

[a] All values are in grams. In addition to the QAS solution and toluene, each mixture contained 5.0 g of HO-PDMS-OH, 0.75 g of MeTAS, and 0.75 g of Cat soln. The "Cat soln." was a 50 mmol solution of TBAF in MIBK.

alkyl amine in a 1.00:0.95 molar ratio. A representative synthetic procedure is as follows: 5.00 g of 3-chloropropyltrimethoxysilane (2.52×10^{-2} moles) and 6.44 g of *N*,*N*-dimethylhexadecylamine (2.39×10^{-2} moles) were mixed thoroughly in a 20 mL scintillation vial. The vial containing the reaction mixture was purged with nitrogen for 5−10 min before sealing the vial. The quaternization reaction was carried out at 110 °C for 48 h using magnetic stirring. After 48 h, the reaction mixture was cooled to room temperature before adding 11.44 g of methanol to produce a 50 wt % solution of hexadecyldimethyl(3-trimethoxysilylpropyl)ammonium chloride (Q-C16-TMS) in methanol. The compositional details for each alkoxysilane-functional QAS synthesis are provided in the Supporting Information, Table S2. Successful alkoxysilane-functional QAS synthesis was confirmed using proton nuclear magnetic resonance (^{1}H NMR) spectroscopy. For each alkoxysilane-functional QAS produced, the ^{1}H NMR spectrum showed complete disappearance of the dimethylamino protons at 2.2 ppm and the appearance of peaks at 3.5 ppm ($-N^+-C\underline{H}_2-$) and 3.3 ppm [$(-N^+-(C\underline{H}_3)_2$] due to quaternization.

Coating Solution Preparation. A modified, automated coating formulation station manufactured by Symyx Discovery Tools, Inc. was used to prepare coating solutions. The modification to the formulation station involved coupling magnets to the stir motors to enable the use of disposable containers and magnetic stirring. Table 1 provides the compositions of each of the coating solutions prepared for the investigation.

Coating Application. Samples for measurements of surface energy (SE) and water contact angle hysteresis (WCAH) as well as surface morphological characterization were prepared using a Gardco applicator. Drawdowns were made over aluminum panels and curing was achieved by allowing the coatings to lie horizontally for 24 h at ambient conditions followed by a 24 h heat treatment at 50 °C using a VWR Asphalt oven to ensure full cure.

For high-throughput (HT) measurements of antifouling (AF) and fouling-release (FR) properties, coating solutions were deposited using an Eppendorf Repeater plus pipetter into wells of 24-well array plates (6 columns and 4 rows) modified with primed aluminum discs in each well. The primer used was Intergard 264. Deposition was done such that a given coating composition occupied three entire columns of the 24-well array plate (12 replicate samples per array plate). The volume of coating solution transferred to each well was 0.25 mL. In addition to the experimental coatings, reference coatings, namely, Intersleek 700, Intersleek 900, and T2 were deposited. Coatings were allowed to cure for 24 h at room temperature and then heated at 50 °C for 24 h to ensure full cure.

Instrumentation. ^{1}H NMR spectra were collected using a JEOL 400 MHz spectrometer and $CDCl_3$ as the lock solvent. A sweep width of 7503 Hz was used with 16,000 data points, resulting in an acquisition time of 2.184 s. Sixteen scans were obtained with a relaxation delay of 4 s.

An automated SE measurement unit manufactured by Symyx Discovery Tools, Inc. and First Ten Angstroms was used to measure coating SE and WCAH. The methods for measuring SE and WCAH are described in detail elsewhere.[18]

Atomic force microscopy (AFM) studies were performed using a Dimension 3100 microscope with a Nanoscope IIIa

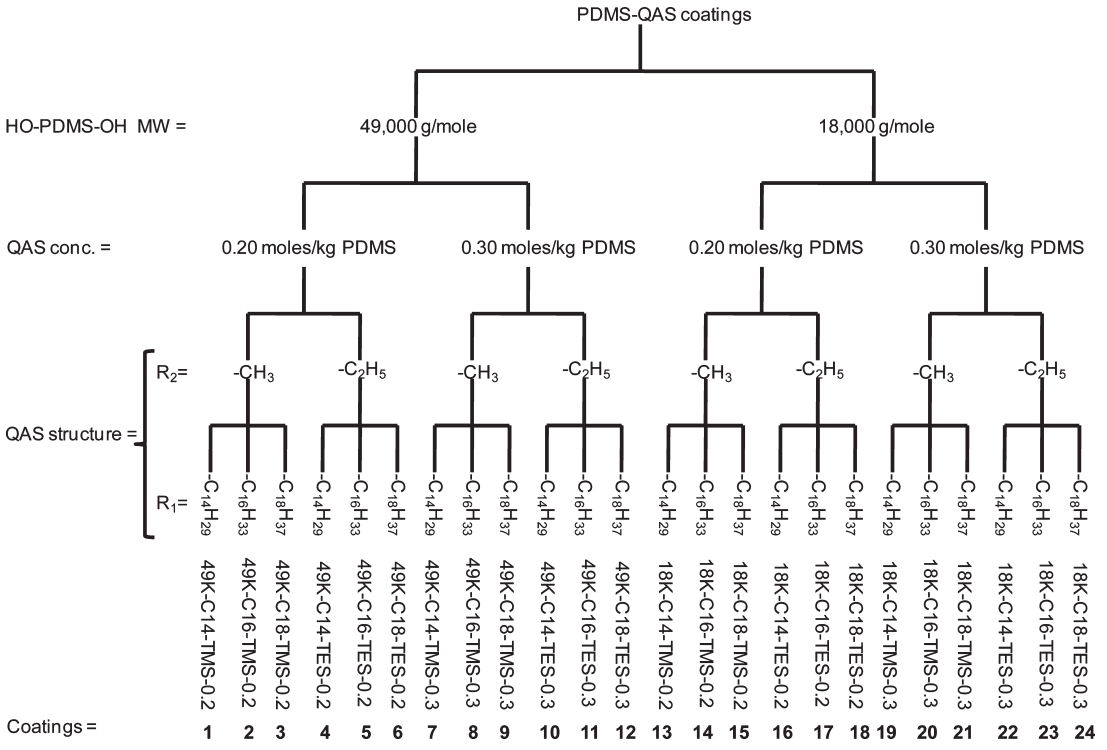

Figure 2. Schematic illustration of the experimental design used for the investigation.

controller from Veeco Incorporated. Images were obtained in tapping mode at ambient conditions using a three-lever silicon probe from MickroMasch. Cantilever length, width, and thickness were $350 \pm 5\,\mu$m, $35 \pm 3\,\mu$m, and $1.7-2.3\,\mu$m, respectively. The spring constant was 0.1−0.4 N/m, resonant frequency 17−24 kHz, and set point ratio 0.8−0.9.

Software. Design-Expert Version 7.0.3 was used to perform ANOVA analyses, and Spotfire DecisionSite 9.1.1 was used to generate scatter plots.

Coating Preconditioning and Cleaning. Prior to the HT assessment of AF and FR properties using marine bacteria and microalgae, coating array plates were immersed in a tap water preconditioning system to remove any leachable, toxic impurities such as solvent, catalyst, or unbound QASs that may influence the measurements. After 35 days of immersion, the array plates were removed from the preconditioning system, and the coating surfaces were immediately cleaned using a semiautomated scrubbing device. The scrubbing device consisted of 24 individually rotating heads that contained disposable, open-cell polyurethane foam tips that fit firmly in the wells of a coating array plate. Each coating array plate was inverted over the foam tips, and pressure was applied until the plate was flush with the Teflon block that houses the rotating heads. A foot switch was then engaged to facilitate scrubbing of each plate for 5 s. Water was forced through each polyurethane foam tip during device operation to maintain cleanliness of the tips and aid in the cleaning process.

HT Assays Based on Microorganisms. After preconditioning and cleaning, the experimental coating compositions were subjected to a leachate toxicity evaluation to ensure that leachable, toxic components were removed from the coatings. The procedure for determining leachate toxicity has been previously described in detail.[20] The HT assessment of AF and FR character using bacteria has previously been described in detail[20,36−39] as have similar HT assays based on microalgae.[20,40] The water-jetting to asses FR character was conducted at 68.95 kpa (10 Psi) and 103.42 kpa (15 Psi) for 5 s toward *C. lytica* and *H. pacifica*, respectively. For *N. incerta*, the water-jetting was conducted at 68.95 kpa (10 Psi) for 10 s.

RESULTS AND DISCUSSION

For the compositional space of interest, described generically in Figure 1, curing and QAS tethering occur by a mixture of condensation reactions involving Si−OH, alkoxysilane, and acetoxysilane groups. Since ambient moisture is involved in the generation of Si−OH groups from alkoxysilane and acetoxysilane groups, this compositional space fits into the general class of polysiloxane-based coatings often referred to as "moisture-cure" or "condensation-cure" coatings.[20,22,41,42] The variables investigated for this study included QAS composition, QAS concentration, and HO-PDMS-OH molecular weight. With regard to QAS composition, R_1 and R_2 were varied. On the basis of previous studies which showed that R_1 chain lengths from 1 to 12 carbon atoms provided little to no enhancement in AF or FR performance,[20,22] the study was limited to R_1 chain lengths ranging from 14 to 18 carbon atoms. R_2 was varied between methyl and ethyl, and HO-PDMS-OH molecular weight was varied at 18,000 and 49,000 g/mol. Figure 2 displays a schematic of the experimental design. A total of 24 unique coating compositions were prepared. The responses measured using HT methods included AF and FR characteristics toward a suite of organisms as well as fundamental surface properties, namely, surface energy (SE) and water contact angle hysteresis (WCAH). Atomic force microscopy (AFM) was conducted on a subset of the coatings prepared.

AF/FR Properties. Three marine microorganisms were used to characterize AF and FR properties. Two of the

dx.doi.org/10.1021/co200004m |*ACS Comb. Sci.* 2011, 13, 298–309

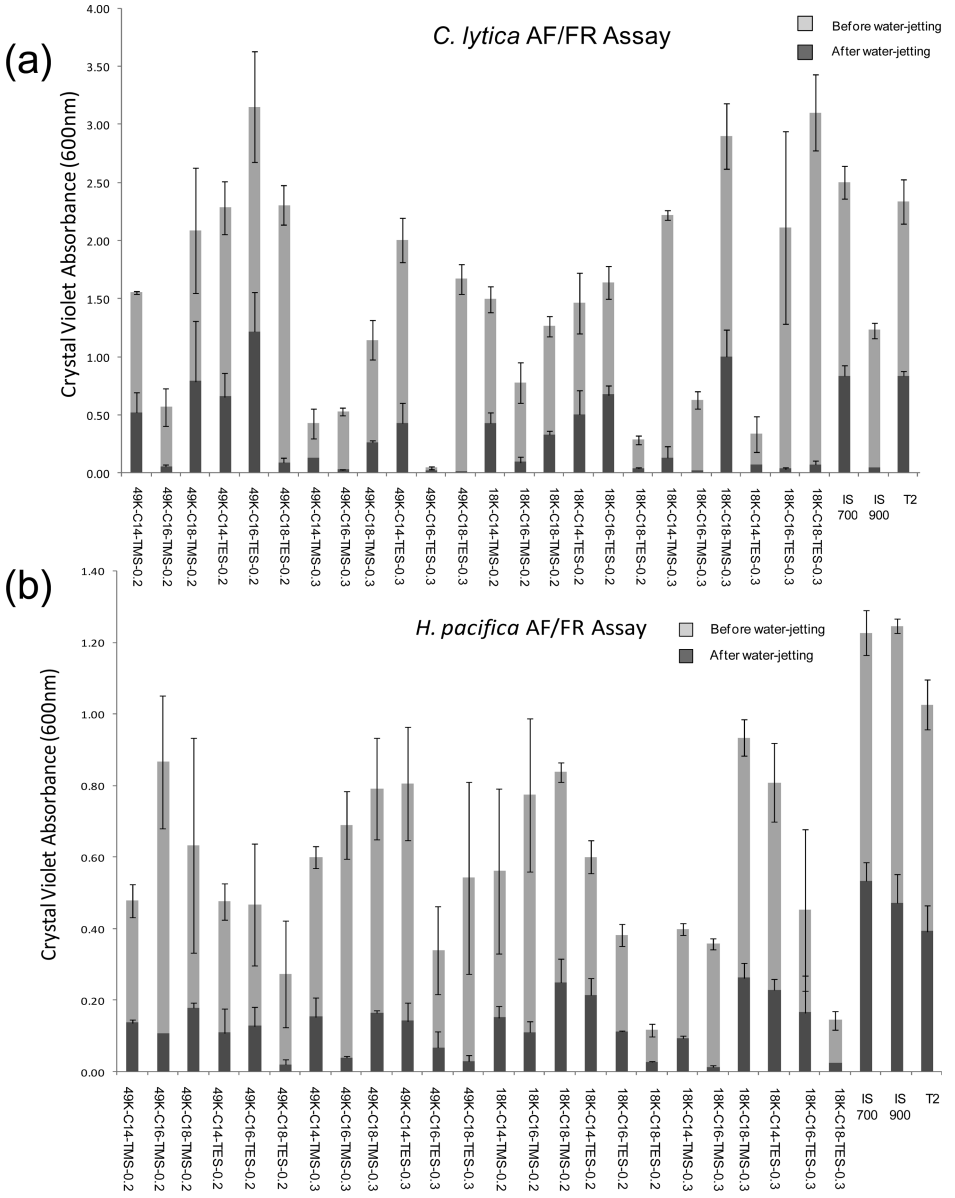

Figure 3. (a) *C. lytica* biofilm retention before and after water-jetting using a pressure of 68.95 kpa. Error bars represent one standard deviation. (b) *H. pacifica* biofilm retention before and after water-jetting using a pressure of 103.42 kpa. Error bars represent one standard deviation.

microorganisms were bacteria, namely, *C. lytica* and *H. pacifica*, while the third was a diatom, *N. incerta*. Figures 3a and 3b display bacterial biofilm retention and removal, while Figure 4 displays diatom attachment and removal for all the experimental coatings and the three different reference coatings (i.e., Intersleek 700, Intersleek 900, and T2). For the two bacterial species, *C. lytica* (Figure 3a) and *H. pacifica* (Figure 3b), the amount of biomass before and after water-jetting is represented by an absorbance value obtained from extraction of the biomass indicator dye from stained biofilms. For the diatom, *N. incerta* (Figure 4), the amount of biomass before and after water-jetting is represented by relative fluorescence units (RFU) obtained from extracting chlorophile from the cells. Casual observation of the plots displayed in Figures 3 and 4 show that a wide variety of responses were obtained from the coatings investigated. For example, considering Figure 3a, sample 49K-C16-TES-0.3 had essentially no biofilm retained on the surface. A response such as this indicates that the coating had good AF character toward *C. lytica*. In contrast, sample 18K-C18-TES-0.3 had a considerable amount of biofilm retained on the surface, but the biofilm was completely removed by the water-jetting process. This response indicates that sample 18K-C18-TES-0.3 had good FR character toward *C. lytica*. For illustration purposes, multiwell plate images of a good AF coating, a good FR coating, and a poor AF/FR coating toward *C. lytica* are provided in the Supporting Information, Figure S1.

To identify statistically significant compositional factors that contribute to enhanced AF and FR character, an ANOVA analysis was conducted. According to the ANOVA analysis of AF behavior (Table S3 in the Supporting Information), R_2 composition was the most significant factor that influenced both *C. lytica* and *H pacifica* biofilm retention. For FR behavior, ANOVA analysis results (Table S3 in the Supporting Information) showed that many of the compositional variables as well as interactions between variables significantly influenced FR

dx.doi.org/10.1021/co200004m |*ACS Comb. Sci.* 2011, 13, 298–309

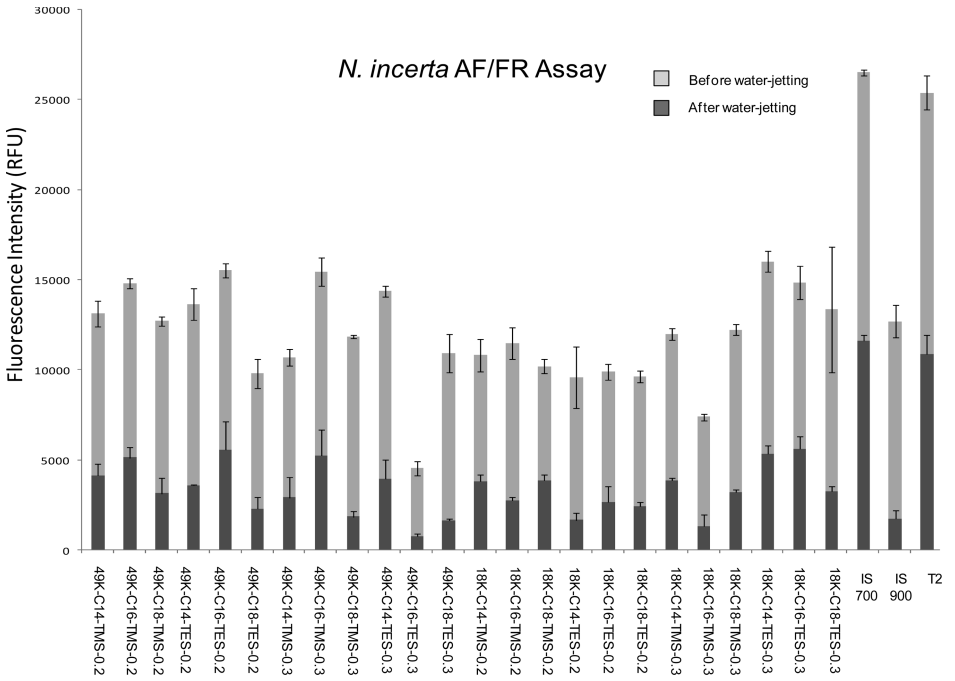

Figure 4. Attached cells of *N. incerta* before and after water jetting using a pressure of 68.95 kpa. Error bars represent one standard deviation.

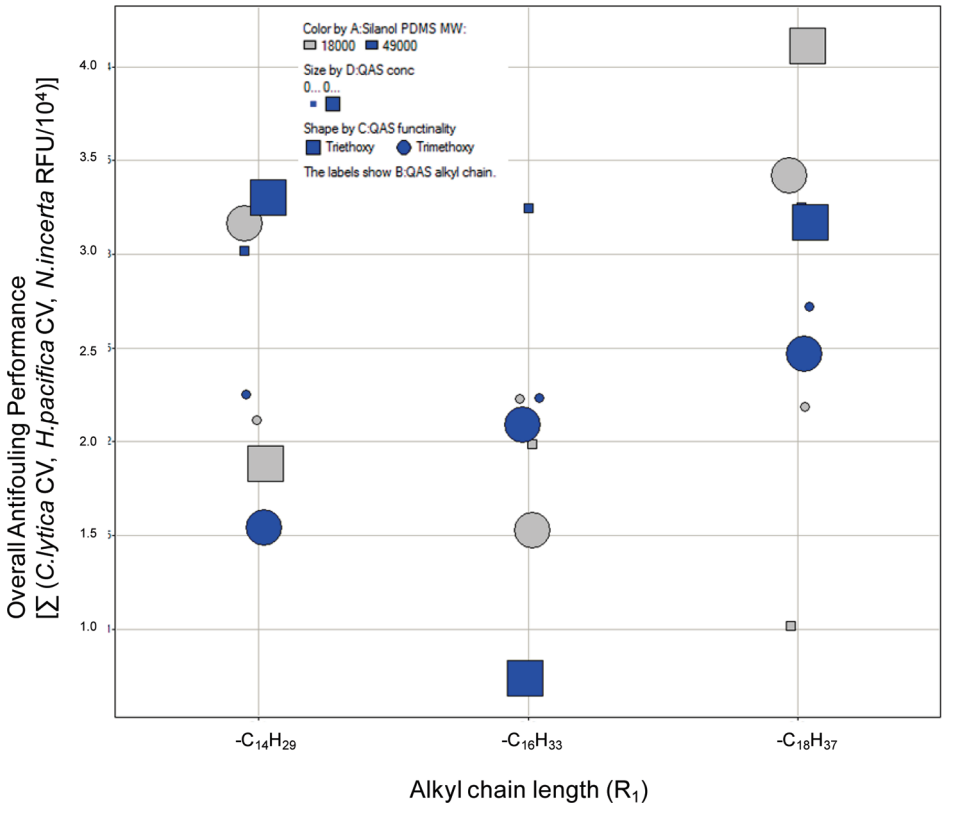

Figure 5. Overall AF activity. The values were generated by summing absorbance values associated with *C. lytica* and *H. pacifica* biomass and fluorescence intensity values associated with *N. incerta* biomass before water-jetting. The RFU values from fluorescence intensity were divided by 10,000 for the calculation of overall AF performance.

performance. For all microorganisms, QAS concentration and R_1 composition was a significant factor either by itself or in an interaction with another variable.

Since there are a tremendous number of fouling species in the world's oceans, it was of interest to identify those compositions and compositional factors that provided "broad-spectrum" AF

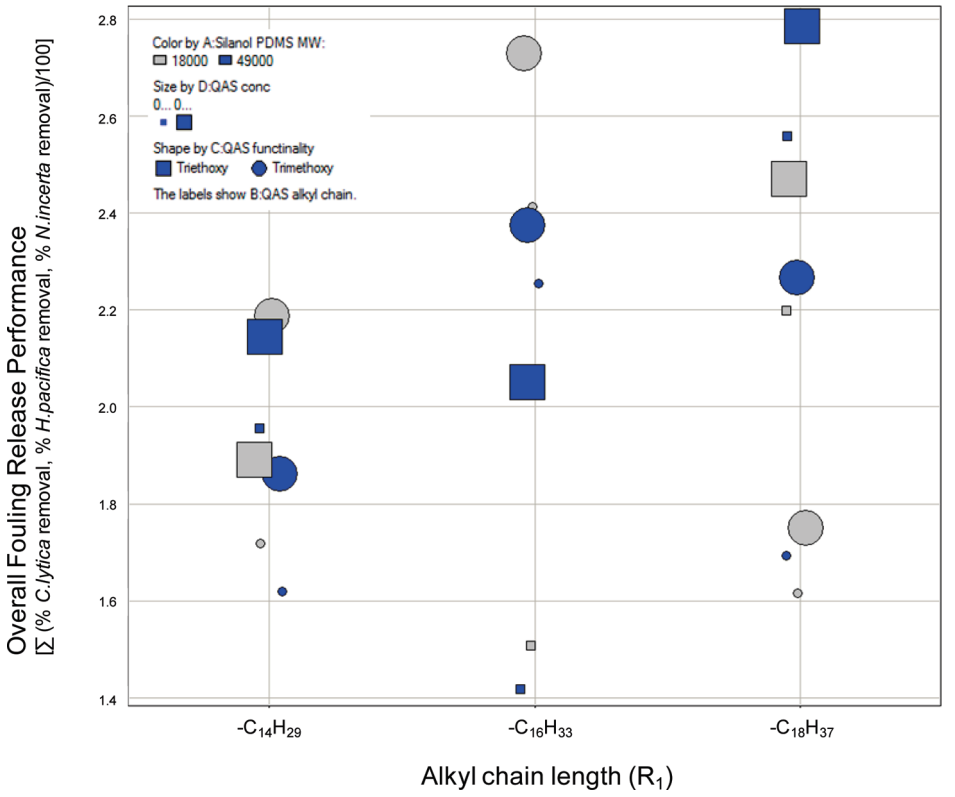

Figure 6. Overall FR activity. The values were generated by summing values of percent biomass removal for *C. lytica*, *H. pacifica*, and *N. incerta*.

and/or FR character. As a result, plots were generated by summing responses from individual microorganisms. Figure 5 was constructed to identify compositional variables that result in good, broad-spectrum AF character. This plot was generated by summing absorbance values associated with *C. lytica* and *H. pacifica* biomass and fluorescence intensity values associated with *N. incerta* biomass before water-jetting. The scatter plot shown in Figure 5 identifies all factors varied in the experiment. The *x*-axis pertains to variations in R_1, the shape of the data symbol pertains to variations in R_2, the size of the data symbol indicates variations in QAS concentration, and the color of the data symbol indicates variation in HO-PDMS-OH molecular weight. Visual inspection of Figure 5 shows that the two coatings that showed the strongest, broad-spectrum AF character were both derived from a QAS with ethoxy silane groups (i.e., $R_2 = -CH_2CH_3$).

Figure 6 displays FR data as a function of the compositional variables by summing values of percent biomass removal for *C. lytica*, *H. pacifica*, and *N. incerta*. Visual inspection of Figure 6 suggests that the higher QAS concentration and R_1 = C16 or C18 results in enhanced FR character.

In addition to analyzing the data according to AF and FR behavior, the data was analyzed based on the amount of biomass remaining after water-jetting. Coatings showing good performance based on this data may exhibit good AF properties, good FR properties, or both good AF and FR properties. Figure 7 was generated by summing absorbance values associated with *C. lytica* and *H. pacifica* biomass and fluorescence intensity values associated with *N. incerta* biomass after water-jetting. Visual inspection of Figure 7 indicates that coatings with R_1 = C16 or C18 and $R_2 = -CH_2CH_3$ generally result in low amounts of biofilm after water-jetting. According to the ANOVA analysis, QAS concentration and an interaction between R_1 and R_2 were the significant terms associated with the amount of biomass remaining after water-jetting.

In addition to developing structure-AF/FR relationships for the compositional space of interest, it was relevant to compare the best performing coatings to a standard polysiloxane coating as well as to commercial, polysiloxane-based FR coatings. Two commercial, polysiloxane-based FR coatings were used for comparison, namely, Intersleek 700 (IS 700) and Intersleek 900 (IS 900). The standard polysiloxane reference coating was T2. T2 is often used by other investigators as a reference for studies of FR properties.[13,15] Figure 8 provides a comparison of AF and FR properties for the best performing experimental coating to IS 700, IS 900, and T2. As shown in Figure 8, the best experimental coating, 49K-C16-TES-0.3, showed much lower initial biomass than the commercial coatings, indicating better AF character for the QAS-containing coating. In addition, water-jetting caused essentially complete removal of the biomass for all three of the microorganisms, indicating excellent FR properties compared to the commercial coatings. It should be understood that the commercial coatings were not designed to exhibit an AF effect; thus, it was not surprising that they did not show a significant inhibition of bacterial biofilm retention or algal cell attachment.

Surface Properties. To obtain some fundamental understanding of the influence of the compositional variables on AF and FR properties, SE and WCAH measurements were made on all of the coatings produced, and AFM was conducted on select coatings possessing systematic variations in composition. Figures S2 and S3 in the Supporting Information display SE and WCAH data, respectively. It can be seen that SE and WCAH varied widely over the compositional space. SEs ranged from 8.3 to 18.3 mN/m. The SEs of most all of the experimental coatings were

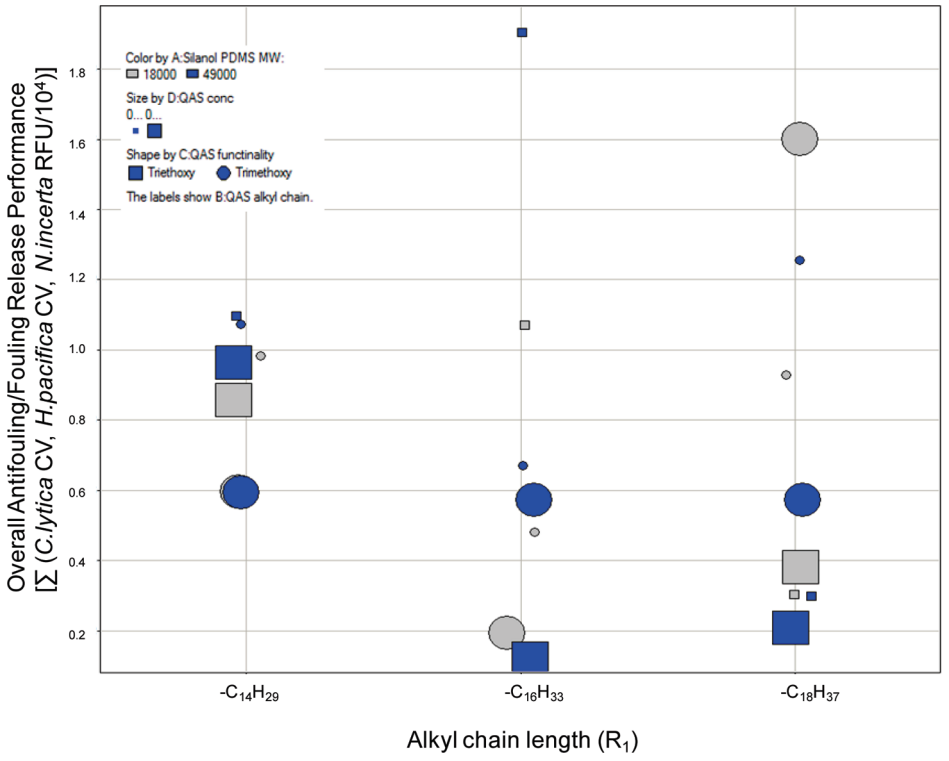

Figure 7. Overall AF/FR activity. The values were generated by summing absorbance values associated with *C. lytica* and *H. pacifica* biomass and fluorescence intensity values associated with *N. incerta* biomass after water-jetting. The RFU values from fluorescence intensity were divided by 10,000 for the calculation of overall AF/FR performance.

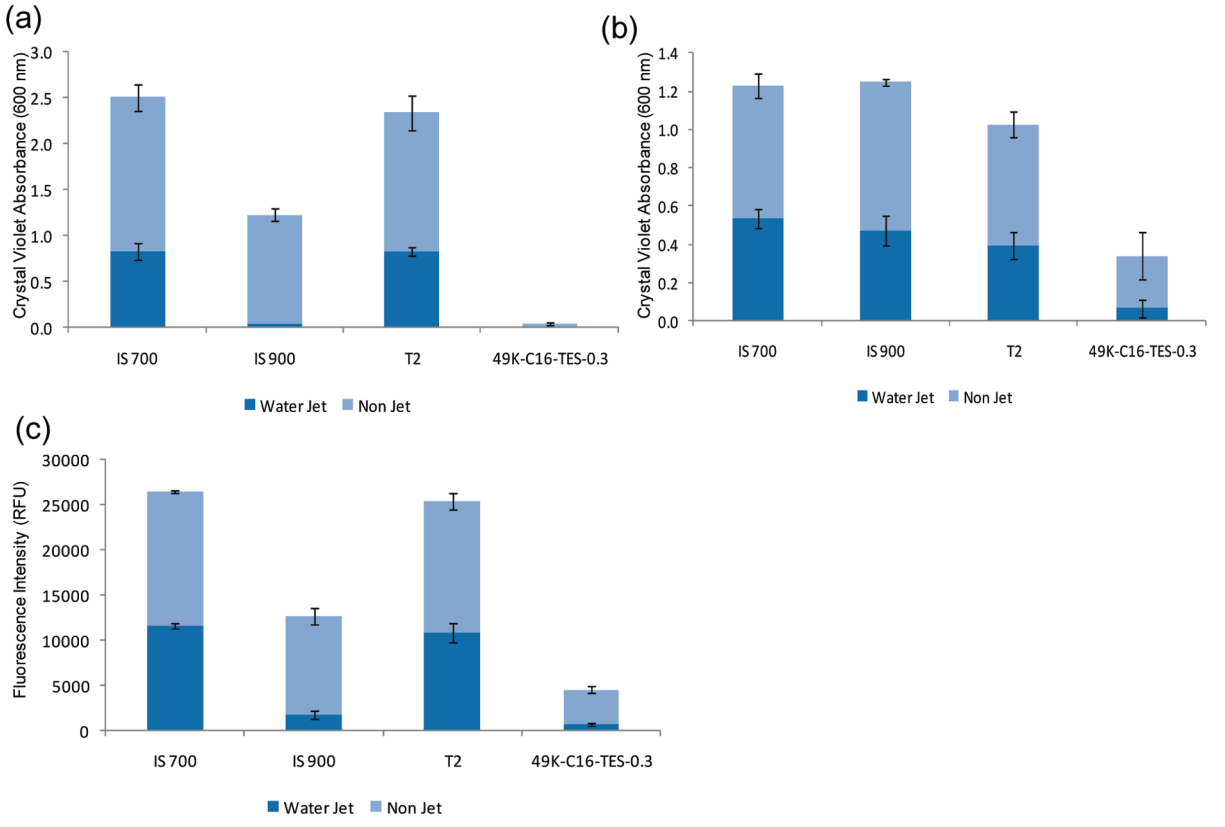

Figure 8. Comparison of AF and FR properties of the best performing experimental coating, 49K-C16-TES-0.3, to the reference coatings, IS 700, IS 900, and T2, toward three microorganisms, (a) *C. lytica*, (b) *H. pacifica*, and (c) *N. incerta*.

dx.doi.org/10.1021/co200004m |*ACS Comb. Sci.* 2011, 13, 298–309

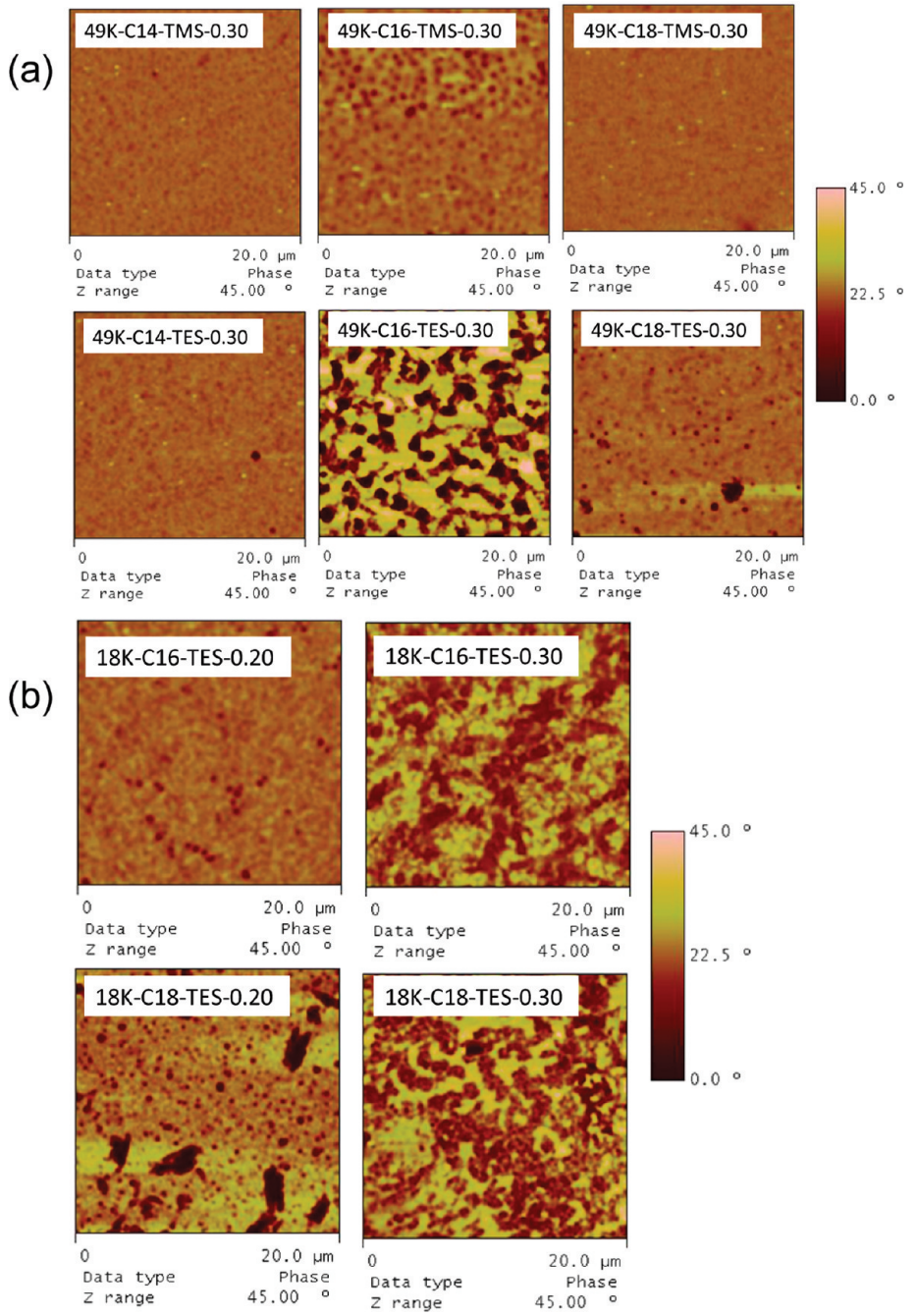

Figure 9. (a) AFM phase images that illustrate the effect of alkoxysilane composition on coating surface morphology. (b) AFM phase images that illustrate the effect of TES-QAS concentration on coating surface morphology.

significantly lower than the 18.2 mN/m value typically reported for PDMS.[20,22] A previous investigation by the authors showed that the lower SEs associated with QAS-functional polysiloxane coatings was due to the formation of a heterogeneous surface morphology composed of QAS-rich surface protrusions which reduced wetting.[20,22] The authors previous investigation also showed that QAS-functional coatings exhibiting a heterogeneous surface morphology exhibited significantly higher WCAH compared to QAS-free analogues. Higher values of WCAH indicate higher surface instability. It was expected that the ionic nature of the QAS groups would provide a significant thermodynamic driving force for surface rearrangement upon exposing the surface to water. The WCAH for the pure polysiloxane reference coating, T2, was 5.3 which is considerably lower than most all of the QAS-functional coatings.

Figure 9 displays AFM images that illustrate the effect of alkoxysilane composition (i.e., ethoxy vs methoxy) and QAS concentration on surface morphology. Since the AFM tip used to generate the images was negatively charged because of an oxide layer with anionic surface functionality, it was expected that considerable contrast would be observed between QAS-rich domains and the siloxane matrix because of the positive charge of the QAS groups. Thus, the darker regions of the phase images were attributed to QAS-rich domains.[43] The AFM images shown

in Figure 9a show an effect on surface morphology resulting from the variation in alkoxysilane composition (i.e., R_2). For the coatings based on R_1 = C16, the surface morphology changed from isolated, circular QAS-rich domains for the coating derived from the TMS-functional QAS (i.e., 49K-C16-TMS-0.30) to highly interconnected QAS domains for the coating derived from the TES-functional QAS (i.e., 49K-C16-TES-0.30). For the coatings based on R_1 = C18, 49K-C18-TES-0.30 showed greater phase contrast compared to 49K-C18-TMS-0.30 indicating a higher surface charge density for the former.

Figure 9b illustrates the effect of increasing the concentration of TES-QAS from 0.20 mol/kg of PDMS to 0.30 mol/kg of PDMS while keeping all other variables constant. Increasing TES-QAS concentration clearly increased the concentration of the QAS-rich phase at the coating surface and changed the surface morphology from isolated QAS-rich domains to highly interconnected QAS-rich domains. These AFM results suggest that the use of TES-QASs as opposed to TMS-QASs results in greater segregation of the QAS groups to the coating/air interface. The production of a higher surface charge density achieved with the use of TES-functional QASs is consistent with the AF and FR results that showed that coatings 49K-C16-TES-0.30 and 49K-C18-TES-0.30 performed considerably better relative to their TMS-QAS-based analogues. The Figure S4 in the Supporting Information further illustrates that the coatings exhibiting the highest AF and FR performance showed a highly heterogeneous surface morphology with relatively large phase contrast compared to a representative coating that exhibited relatively poor AF and FR properties.

The final surface morphology of these "moisture-cure" or "condensation-cure" QAS-tethered polysiloxane coatings results from complex interactions between various parameters such as rate of cross-linking, rate of solvent evaporation, increase in viscosity during film formation, and their effect on thermodynamic driving force of phase separation between polar QAS molecules and nonpolar PDMS. The higher extent of QAS surface segregation achieved with the use of TES-functional QASs as compared to analogous TMS-functional QASs may be attributed to their relative differences in reactivity. During substitution reactions ethoxysilane groups provide more steric hindrance compared to methoxysilane groups while $-OCH_2CH_3$, generated during hydrolysis of ethoxysilane, is a poor leaving group compared to $-OCH_3$. Hence, ethoxysilane groups are less reactive toward hydrolysis and substitution reactions compared to methoxysilane groups.[44,45] Since cross-linking and tethering of QAS groups to the cross-linked network occurs during the process of film formation, the slower reaction rate of the TES-functional QASs may provide additional time for diffusion to the coating-air interface before being incorporated into the cross-linked network.

CONCLUSION

As a result of extensive studies using a C/HT approach, it has been demonstrated that the AF and FR properties of moisture-curable polysiloxanes based on a QAS-functional silane depend strongly on multiple compositional variables.[35−37] This particular study involved a variable that had not been previously studied, namely, the chemical composition of the alkoxy group on the QAS-functional alkoxysilane (R_2 in Figure 1). It was found that utilization of ethoxysilane-functional QASs provided better AF character than their methoxysilane-functional analogues. The study also showed that other variables such as QAS concentration, alkyl group attached to the QAS nitrogen atom (R_1 in Figure 1), and their interactions with R_2 had significant effect on AF/FR character of the coatings. Coating compositions containing ethoxysilane-functional QAS with $R_1 \geq$ C16 and at higher QAS concentration would minimize the biomass remaining after water-jetting. A comparison of the best performing experimental coating, 49K-C16-TES-0.3, to the commercial FR coatings, IS 700 and IS 900, showed that the experimental coating resulted in much lower biomass retention for all three microorganisms than the commercial FR coatings, and the biomass that was retained was essentially completely removed by water-jetting. Results obtained with AFM showed enhanced segregation of QAS groups to the coating-air interface resulting from the use of ethoxysilane-functional QASs as compared to methoxysilane-functional QASs. It was hypothesized that the higher concentration of QAS groups at the coating-air interface observed for ethoxysilane-functional QASs resulted from slower kinetics of hydrolysis and condensation reactions associated with ethoxysilane groups as compared to methoxysilane groups. A slower reaction rate would be expected to allow more time for diffusion of the QAS-functional silane to the coating-air interface before it becomes incorporated into the developing cross-linked polymer network.

ASSOCIATED CONTENT

Supporting Information. Tables describing details of the starting materials, compositions of the alkoxysilane-functional QASs, and ANOVA analysis. Figures illustrating the images of experimental coatings in multiwell plates before and after water-jetting, SE data, WCAH data, and AFM phase images of a good AF coating, a good FR coating, and a poor AF/FR coating. This material is available free of charge via the Internet at http://pubs.acs.org.

AUTHOR INFORMATION

Corresponding Author

*E-mail: partha.majumdar@ndsu.edu. Phone: +1-701-231-5357. Fax: +1-701-231-5325.

ACKNOWLEDGMENT

The authors acknowledge financial support from the Office of Naval Research through Grants N00014-05-1-0822 and N00014-06-1-0952.

REFERENCES

(1) Yebra, D. M.; Kiil, S.; Dam-Johansen, K. Antifouling technology-past, present and future steps towards efficient and environmentally friendly antifouling coatings. *Prog. Org. Coat.* **2004**, *50*, 75–104.

(2) Marechal, J.-P.; Hellio, C. Challenges for the development of new non-toxic antifouling solutions. *Int. J. Mol. Sci.* **2009**, *10* (11), 4623–4637.

(3) Grozea, C. M.; Walker, G. C. Approaches in designing non-toxic polymer surfaces to deter marine biofouling. *Soft Matter* **2009**, *5*, 4088–4100.

(4) Schultz, M. P. Effects of coating roughness and biofouling on ship resistance and powering. *Biofouling* **2007**, *23*, 331–341.

(5) Dobretsov, S.; Dahms, H.-U.; Qian, P.-Y. Inhibition of biofouling by marine microorganisms and their metabolites. *Biofouling* **2006**, *22*, 43–54.

(6) Kiil, S.; Weinell, C. E.; Pedersen, M. S.; Dam-Johansen, K.; Codolar, S. A. Dynamic simulations of a self-polishing antifouling paint exposed to seawater. *J. Coat. Technol.* **2002**, *74* (929), 45–54.

(7) Kiil, S.; Weinell, C. E.; Pedersen, M. S.; Dam-Johansen, K. Analysis of self-polishing antifouling paints using rotary experiments and mathematical modeling. *Ind. Eng. Chem. Res.* **2001**, *40* (18), 3906–3920.

(8) Strand, J.; Jacobsen, J. A. Accumulation and trophic transfer of organotins in a marine food web from the Danish coastal waters. *Sci. Total Environ.* **2005**, *350*, 72–85.

(9) Strand, J.; Jacobsen, J. A.; Pedersen, B.; Granmo, A. Butyltin compounds in sediment and molluscs from the shipping strait between Denmark and Sweden. *Environ. Pollut.* **2003**, *124*, 7–15.

(10) Brady, R F., Jr. Clean hulls without poisons: devising and testing nontoxic marine coatings. *J. Coat. Technol.* **2000**, *72*, 44–56.

(11) Brady, R F., Jr.; Singer, I L. Mechanical factors favoring release from fouling release coatings. *Biofouling* **2000**, *15* (1−3), 73–81.

(12) Brady, R. F., Jr. Properties which influence marine fouling resistance in polymers containing silicon and fluorine. *Prog. Org. Coat.* **1999**, *35*, 31–35.

(13) Krishnan, S.; Wang, N.; Ober, C. K.; Finlay, J. A.; Callow, M. E.; Callow, J. A.; Hexemer, A.; Sohn, K. E.; Kramer, E. J.; Fischer, D. A. Comparison of the fouling release properties of hydrophobic fluorinated and hydrophilic PEGylated block copolymer surfaces: attachment strength of the diatom *Navicula* and the green alga *Ulva*. *Biomacromolecules* **2006**, *7*, 1449–1462.

(14) Statz, A.; Finlay, J.; Dalsin, J.; Callow, M.; Callow, J. A.; Messersmith, P. B. Algal antifouling and fouling-release properties of metal surfaces coated with a polymer inspired by marine mussels. *Biofouling* **2006**, *22*, 391–399.

(15) Krishnan, S.; Ayothi, R.; Hexemer, A.; Finlay, J. A.; Sohn, K. E.; Perry, R.; Ober, C. K.; Kramer, E. J.; Callow, M. E.; Callow, J. A.; Fisher, D. A. Anti-biofouling properties of comblike block copolymers with amphiphilic side chains. *Langmuir* **2006**, *22* (11), 5075–5086.

(16) Carman, M.; Estes, T.; Feinberg, A.; Schumacher, J.; Wilkerson, W.; Wilson, L.; Callow, M.; Callow, J.; Brennan, A. Engineered antifouling microtopographies--correlating wettability with cell attachment. *Biofouling* **2006**, *22*, 11–21.

(17) Schumacher, J. F.; Carman, M. L.; Estes, T. G.; Feinberg, A. W.; Wilson, L. H.; Callow, M. E.; Callow, J. A.; Finlay, J. A.; Brennan, A. B. Engineered antifouling microtopographies - effect of feature size, geometry, and roughness on settlement of zoospores of the green alga *Ulva*. *Biofouling* **2007**, *23*, 55–62.

(18) Majumdar, P.; Stafslien, S.; Daniels, J.; Webster, D. C. High throughput combinatorial characterization of thermosetting siloxane-urethane coatings having spontaneously formed microtopographical surfaces. *J. Coat. Technol. Res.* **2007**, *4* (2), 131–138.

(19) Webster, D. C.; Chisholm, B. J. New directions in antifouling technology. In *Biofouling*; Duerr, S., Thomason, J. C., Eds.; John Wiley & Sons Ltd.: U.K., 2010; pp 366−387.

(20) Majumdar, P.; Lee, E.; Patel, N.; Ward, K.; Stafslien, S. J.; Daniels, J.; Chisholm, B. J.; Boudjouk, P.; Callow, M. E.; Callow, J. A.; Thompson, S. E. M. Combinatorial materials research applied to the development of new surface coatings IX: an investigation of novel antifouling/fouling-release coatings containing quaternary ammonium salt groups. *Biofouling* **2008**, *24* (3), 185–200.

(21) Majumdar, P.; Lee, E.; Patel, N.; Stafslien, S. J.; Daniels, J.; Chisholm, B. J. Development of environmentally friendly, antifouling coatings based on tethered quaternary ammonium salts in a crosslinked polydimethylsiloxane matrix. *J. Coat. Technol. Res.* **2008**, *5* (4), 405–417.

(22) Majumdar, P.; Lee, E.; Gubbins, N.; Christianson, D. A.; Stafslien, S. J.; Daniels, J.; VanderWal, L.; Bahr, J.; Chisholm, B. J. Combinatorial materials research applied to the development of new surface coatings XIII: an investigation of polysiloxane antimicrobial coatings containing tethered quaternary ammonium salt groups. *J. Comb. Chem.* **2009**, *11* (6), 1115–1127.

(23) Tashiro, T. Antibacterial and bacterium adsorbing macromolecules. *Macromol. Mater. Eng.* **2001**, *286*, 63–87.

(24) Ioannou, C. J.; Hanlon, G. W.; Denyer, S. P. Action of disinfectant quaternary ammonium compounds against *Staphylococcus aureus*. *Antimicrob. Agents Chemother.* **2007**, *51* (1), 296–306.

(25) Majumdar, P.; Lee, E.; Gubbins, N.; Stafslien, S. J.; Daniels, J.; Thorson, C. J.; Chisholm, B. J. Synthesis and antimicrobial activity of quaternary ammonium-functionalized POSS (Q-POSS) and polysiloxane coatings containing Q-POSS. *Polymer* **2009**, *50* (5), 1124–1133.

(26) Sauvet, G.; Fortuniak, W.; Kazmierski, K.; Chojnowski, J. Amphiphilic block and statistical siloxane copolymers with antimicrobial activity. *J. Polym. Sci., Part A: Polym. Chem.* **2003**, *41* (19), 2939–2948.

(27) Gottenbos, B.; van der Mei, H. C.; Klatter, F.; Nieuwenhuis, P.; Busscher, H. J. In vitro and in vivo antimicrobial activity of covalently coupled quaternary ammonium silane coatings on silicone rubber. *Biomaterials* **2002**, *23* (6), 1417–1423.

(28) Kuegler, R.; Bouloussa, O.; Rondelez, F. Evidence of a charge-density threshold for optimum efficiency of biocidal cationic surfaces. *Microbiology* **2005**, *151* (5), 1341–1348.

(29) Murata, H.; Koepsel, R. R.; Matyjaszewski, K.; Russell, A. J. Permanent, non-leaching antibacterial surfaces-2: how high density cationic surfaces kill bacterial cells. *Biomaterials* **2007**, *28* (32), 4870–4879.

(30) Chisholm, B.; Potyrailo, R.; Cawse, J.; Shaffer, R.; Brennan, M.; Molaison, C.; Whisenhunt, D.; Flanagan, B.; Olson, D.; Akhave, J.; Saunders, D.; Mehrabi, A.; Licon, M. The development of combinatorial chemistry methods for coating development I. Overview of the experimental factory. *Prog. Org. Coat.* **2002**, *45*, 313–321.

(31) Chisholm, B.; Potyrailo, R.; Cawse, J.; Shaffer, R.; Brennan, M.; Molaison, C. Combinatorial chemistry methods for coating development. IV. The importance of understanding process capability. *Prog. Org. Coat.* **2003**, *47*, 120–127.

(32) Webster, D. C.; Chisholm, B. J.; Stafslien, S. J. Mini-review: combinatorial approaches for the design of novel coating systems. *Biofouling* **2007**, *23*, 179–192.

(33) Chisholm, B. J.; Stafslien, S. J.; Majumdar, P.; Webster, D. Automated process speed up development of marine antifouling coatings. *Eur. Coat. J.* **2008**, *11*, 32–37.

(34) Webster, D. C.; Bennett, J.; Kuebler, S.; Kossuth, M. B.; Jonasdottir, S. High throughput workflow for the development of coatings. *J. Coat. Technol.* **2004**, *1* (6), 34–39.

(35) Holland, R.; Dugdale, T. M.; Wetherbee, R.; Brennan, A. B.; Finlay, J. A.; Callow, J. A.; Callow, M. Adhesion and motility of fouling diatoms on a silicone elastomer. *Biofouling* **2004**, *20*, 323–329.

(36) Kugel, A. J.; Jarabek, L. E.; Daniels, J. W.; Vander Wal, L. J.; Ebert, S. M.; Jepperson, M. J.; Stafslien, S. J.; Pieper, R. J.; Webster, D. C.; Bahr, J.; Chisholm, B. J. Combinatorial materials research applied to the development of new surface coatings XII: Novel, environmentally friendly antimicrobial coatings derived from biocide-functional acrylic polyols and isocyanates. *J. Coat. Technol. Res.* **2009**, *6*, 107–121.

(37) Stafslien, S.; Daniels, J.; Chisholm, B.; Christianson, D. Combinatorial materials research applied to the development of new surface coatings III. Utilization of a high-throughput multiwell plate screening method to rapidly assess bacterial biofilm retention on antifouling surfaces. *Biofouling* **2007**, *23*, 37–44.

(38) Stafslien Shane, J.; Bahr James, A.; Daniels Justin, W.; Wal Lyndsi, V.; Nevins, J.; Smith, J.; Schiele, K.; Chisholm, B. Combinatorial materials research applied to the development of new surface coatings VI: An automated spinning water jet apparatus for the high-throughput characterization of fouling-release marine coatings. *Rev. Sci. Instrum.* **2007**, *78*, 072204.

(39) Stafslien, S. J.; Bahr, J. A.; Feser Jason, M.; Weisz, J. C.; Chisholm, B. J.; Ready, T. E.; Boudjouk, P. Combinatorial materials research applied to the development of new surface coatings I: a multiwell plate screening method for the high-throughput assessment of bacterial biofilm retention on surfaces. *J. Comb. Chem.* **2006**, *8*, 156–162.

(40) Casse, F.; Stafslien, S. J.; Bahr, J. A.; Daniels, J.; Finlay, J. A.; Callow, J. A.; Callow, M. E. Combinatorial materials research applied to the development of new surface coatings V. Application of a spinning

water-jet for the semi-high throughput assessment of the attachment strength of marine fouling algae. *Biofouling* **2007**, *23*, 121–130.

(41) Andersson, L. H. U.; Hjertberg, T. J. Silicone elastomers for electronic applications. I. Analyses of the noncrosslinked fractions. *J. Appl. Polym. Sci.* **2003**, *88*, 2073–2081.

(42) de Buyl, F. Silicone sealants and structural adhesives. *Int. J. Adhes. Adhes.* **2001**, *21*, 411–422.

(43) Tan, S.; Sherman, R. L., Jr.; Qin, D.; Ford, W. T. Surface heterogeneity of polystyrene latex particles determined by dynamic force microscopy. *Langmuir* **2005**, *21* (1), 43–49.

(44) Altmann, S.; Pfeiffer, J. Hydrolysis/condensation behavior of alkoxy[(methacryloyloxy)alkyl]silanes: structure-reactivity relations. *Monatsh. Chem.* **2003**, *134*, 1081–1092.

(45) Osterholtz, F. D.; Pohl, E. R. Kinetics of the hydrolysis and condensation of organofunctional alkoxysilanes: a review. *J. Adhes. Sci. Technol.* **1992**, *6* (1), 127–149.